Journal of Materials Chemistry

PAPER

A new supramolecular film formed from a silsesquioxane derivative for application in proton exchange membranes†

Chih-Chia Cheng, Ying-Chieh Yen, Fu-Hsiang Ko, Chih-Wei Chu, Shih-Kang Fan and Feng-Chih Chang*

A new polyhedral oligomeric silsesquioxane ionomer (HCl-doped POSS-C11-Py) has been investigated. This new ionomer is able to self-assemble through macromers by quadruple hydrogen bonding interactions into a physically crosslinked polymer-like material that can be easily fabricated into films with micro-phase separation. This HCl-doped POSS-C11-Py membrane exhibits higher proton conductivity than a typical Nafion® membrane at high temperature, which is extremely rare for a non-sulfonic acid system. This newly developed material may provide an alternative route toward design and fabrication of a new type of proton exchange membranes.

Introduction

Supramolecular self-assembly has attracted great attention because of the novel structural organizations formed through highly complementary molecular recognition events.[1] A typical example is the assembly and disassembly of structural motifs such as DNA and RNA—fundamental of translation and transcription in biology—offering unique opportunities for enhanced control of self-assembly.[2] Noncovalent interactions such as hydrogen bonding, ionic interactions, metal coordination, electrostatic interactions, and π–π stacking have been used individually or in concert with one another to obtain well-controlled and reliable properties such as high specificity, controlled affinity, and spontaneous self-assembly behavior.[3a] Nevertheless, it is still a challenge to control the supramolecular materials with secondary (and higher) bonding through specific interactions.[3b] Recently, several supramolecular structures have been incorporated into polymers[4] to form materials with features of conventional polymers and reversibility in the bonding between monomer units.[5] Chemists started to learn how to mimic the natural use of noncovalent chemistry in polymer science and harnessed these interesting biomolecules to construct complex nanostructures and materials in the foundation of supramolecular polymer science.

Polyhedral oligomeric silsesquioxanes (POSSs), $(RSiO_{1.5})_n$, are intermediates between silica (SiO_2) and silicone (R_2SiO), comprising a hydrophobic inorganic core covered externally by organic substituents.[6] Recently, organic/inorganic hybrid nanocomposites based on POSS derivatives have attracted considerable interest because they exhibit several advantageous

properties resulting from the unique physical properties of POSS nanoparticles.[7] Through appropriate design of their architectures, POSS derivatives can be tailored for specific applications.[8] POSS hybrid materials are potential candidates for use in proton exchange membranes (PEMs) but only a few reports have been published.[9] The relatively hydrophobic POSS core as compared with sulfonated materials and adjustable external functionalities are able to affect the water behavior and dimensional stability.

In our previous study, we found that uracil-terminated telechelic sulfonated polyimides can be transformed into noncovalent network membranes through biocomplementary hydrogen bonding recognition in the presence of an adenine-based crosslinking agent, thereby providing an alternative route to design new PEMs from supramolecular polymers.[10] Recently, we reported a new POSS macromer with quadruple hydrogen bonding interactions and its formation of a physically cross-linked polymer-like structure with good mechanical properties (tensile strength = 46.1 MPa, tensile modulus = 0.58 GPa, elongation = 49.3%).[11] This study further demonstrates that this macromer can be used in the PEM, which is probably the first example of the supramolecular network PEM formed by the assembly of self-complementary low molecular-weight macromer. More surprisingly, we also found that this membrane exhibited slightly higher proton conductivity than Nafion®-117 at high temperature and relative humidity.

Results and discussion

A physically cross-linked POSS derivative, POSS-C11-Py, thin film was prepared according to our previous report.[11] The thin film was further reacted with aqueous hydrochloric acid to form ammonium and amine chloride ionomer (Scheme 1). In other words, amine and pyridine groups readily react with dilute acids to give the corresponding acid–base composite salt. After HCl treatment, the HCl-doped POSS-C11-Py thin film can retain its

Institute of Applied Chemistry, National Chiao-Tung University, 30050 Hsinchu, Taiwan. E-mail: changfc@mail.nctu.edu.tw; Fax: +886-3-5131512; Tel: +886-3-5131512
† Electronic supplementary information (ESI) available. See DOI: 10.1039/c1jm12929e
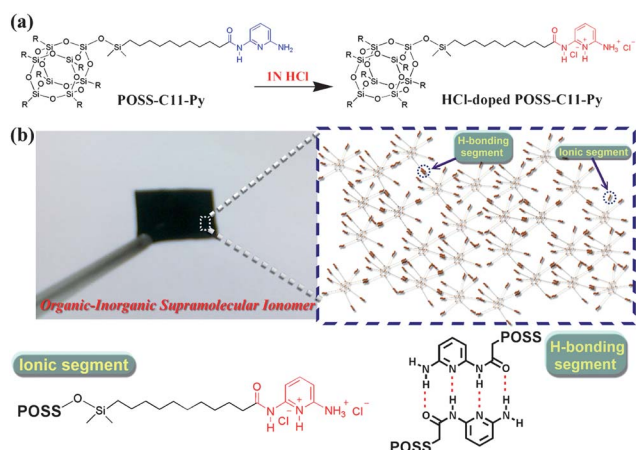
Scheme 1 (a) Synthesis of the HCl-doped POSS-C11-Py membrane. (b) Photographic image and graphical representations of a supramolecular ionomer formed from the HCl-doped POSS-C11-Py membrane.

shape at low relative humidity (RH) (<30%) but becomes brittle, whereas the film stored at high RH (>70%) remains flexible. The water which is absorbed when the RH is increased acts as a "plasticizer", decreasing the electrostatic interactions such as ionic or hydrogen bonding. This intriguing behavior leads us to investigate the phase transitions in the films in more detail through DSC measurements. Differential scanning calorimetry (DSC) analyses of POSS-C11-Py and HCl-doped POSS-C11-Py films provided insight into the behavior of their molecular motion temperature (Fig. 1). The DSC trace of POSS-C11-Py films shows one glass transition (T_g) at 38 °C, implying that a highly self-supporting complementary hydrogen bonding system existed.[11] Surprisingly, the HCl-doped POSS-C11-Py film exhibits two T_gs at 69 and 172 °C, both are higher than that of the POSS-C11-Py film, indicating the presence of micro-phase separation. The T_g at 172 °C comes from the ionic bonded amorphous phase as shown in Scheme 1, implying that the hydrogen bonded dominant phase is excluded and results in two glass transition temperatures. To further confirm the DSC results, we performed small and wide-angle X-ray scattering (SAXS and WAXS) experiments to analyze the microstructure of these POSS derivatives (Fig. 2). The SAXS profiles indicate that
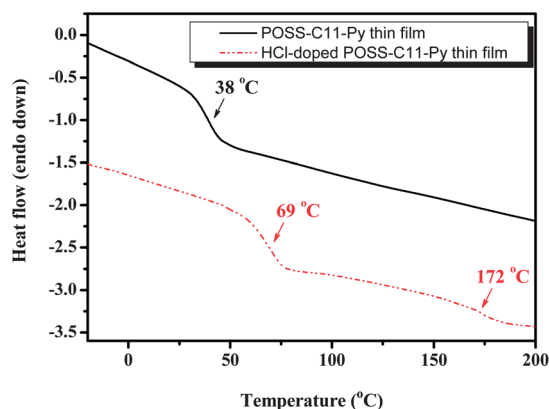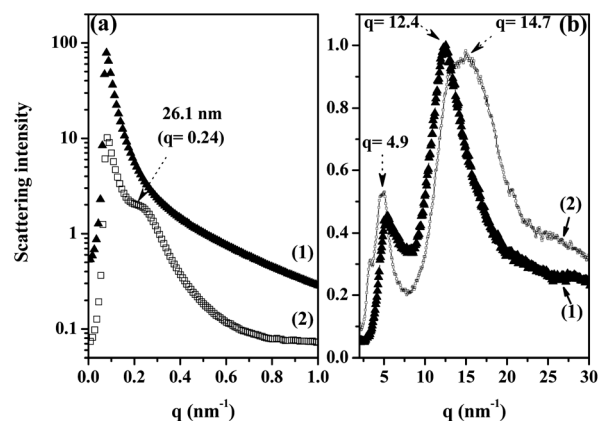

Fig. 2 (a) SAXS and (b) WAXS data for (1) POSS-C11-Py and (2) HCl-doped POSS-C11-Py membranes recorded at room temperature.

the HCl-doped POSS-C11-Py film has a long period of *ca.* 26.1 nm (0.24 nm^{-1}), which is also obviously different from the pure POSS-C11-Py film (Fig. 2a). Based on DSC and X-ray analyses, the HCl-doped POSS-C11-Py film possesses micro-phase separation behavior in the bulk state. In addition, the HCl-doped POSS-C11-Py film also possesses a peak at 4.9 nm^{-1}, implying that the strong complementary quadruple hydrogen bonding interactions are mostly retained after HCl-doping, which has rarely been observed.[11] Moreover, the HCl-doped POSS-C11-Py film exhibits an obvious shift of q (from 12.4 to 14.7 nm^{-1}) corresponding to its intramolecular amorphous region as shown in Fig. 2b, indicative of unspecified structural features at a relatively small cluster size and the connectivity between different ionic clusters. By comparing the amorphous halos corresponding to inter- and intrachain distances of the POSS-C11-Py and HCl-doped POSS-C11-Py films, the introduction of ionic inter-actions results in extending the intramolecular spacing and reducing the intermolecular distance between ionic domains and the formation of physical network of these domains. In addition, TGA curves (see ESI, Fig. S3†) suggest that the HCl-doped procedure does not affect the thermal property of the HCl-doped POSS-C11-Py because of its high decomposition temperature ($T_{d,5\%}$ = 320 °C).

To further understand the physical cross-linking density, we examined the ion exchange capacity (IEC) to estimate the extent of hydrogen-bonding interactions in the HCl-doped POSS-C11-Py film, *i.e.*, the presence of ammonium and amine chloride units in the thin film. The calculated IEC value of the thin film was *ca.* 1.01 ± 0.5 mequiv. g^{-1} (5 samples). Comparison with the theoretical IEC value of 4.1 mequiv. g^{-1} indicates that the physical cross-linking density was as high as 75%. This film has a similar IEC value to Nafion®-117 (0.91 mequiv. g^{-1}), good film-forming property, and good balance between mechanical strength and acid-doping level capacity. Furthermore, we examined the film's oxidation stability by subjecting it to Fenton's reagent [30% H_2O_2 containing $FeSO_4$ (2 ppm)] at 80 °C. After 17 h of test, the HCl-doped POSS-C11-Py film started to break, however, it was still able to withstand the solution for up to 6 months, confirming its excellent chemical stability in fuel cell applications.

From measurements of the proton conductivity of the HCl-doped POSS-C11-Py thin film placed in a closed cell at 90%

Fig. 1 DSC curves of POSS-C11-Py and HCl-doped POSS-C11-Py membranes.
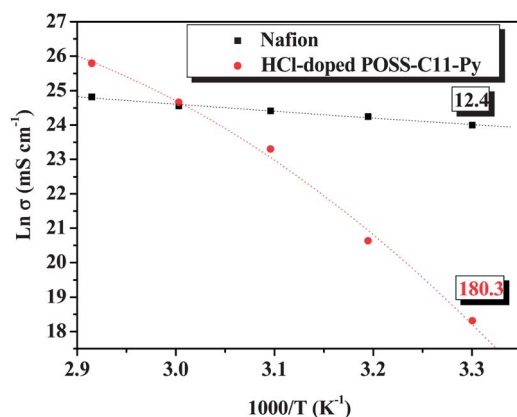
Fig. 3 Temperature dependence of the proton conductivities of the HCl-doped POSS-C11-Py membrane and Nafion®-117 at 90% relative humidity.

relative humidity, a positive temperature–conductivity dependency was observed (Fig. 3). At 70 °C, the HCl-doped POSS-C11-Py thin film exhibits a high conductivity of 25.7 mS cm⁻¹, slightly higher than the Nafion® (24.8 mS cm⁻¹) under the same conditions. The calculated activation energy (E_a) from the Arrhenius plots[12] of the conductivities is 180.3 kJ mol⁻¹, which is similar to other reported hydrous proton conductors.[13a,b] The high activation energy provides additional potential for the existence of oxidation-inhibiting character in fuel cells.[13c] The proton transfer obeys the Grotthuss mechanism,[13d] revealing that the protons jump from one water molecule to the next through hydrogen bonds. On the other hand, this membrane exhibits substantially higher water uptake (63%) relative to that of the Nafion® membrane (35%) due to greater separation of its hydrophilic domains.[14] The physical properties of the POSS-based film, particularly its water sorption and comparable conductivity to the Nafion®, suggest its potential applications in high-temperature fuel cells. High-temperature fuel cells derived from the non-sulfonic acid system are extremely rare, thus, we are encouraged to study the shape[15] and pK_a value[15c] of this material in the future because these factors generally have a dramatic effect on proton conductivity.

Conclusions

In summary, we prepared a new supramolecular ionomer (HCl-doped POSS-C11-Py) possessing quadruple hydrogen-bonding and ionic side arms. The hierarchical control of these interactions between well-defined self-assembled arrays within this supramolecule results in dramatic changes in micro-phase separation behavior, allowing us to fabricate self-supporting films from the supramolecule. In addition, the proton conductivity and water uptake of the HCl-doped POSS-C11-Py thin film are higher as compared with Nafion® at high temperatures.

Experimental

Preparation of the HCl-doped POSS-C11-Py membrane

The flexible POSS-C11-Py film[11] was prepared by casting the DMF solution of POSS-C11-Py onto a smooth glass substrate,

air-drying and thermally annealing at 150 °C. The resultant film was maintained for at least one week at room temperature to make certain the completion of the transition of hydrogen bonding interactions. The membrane was removed from the glass by soaking it in deionized water. After immersion in 1 N HCl for 24 h, the film was obtained in acidic form, washed with deionized water until the pH reached 6–7. The membrane was stored in water at room temperature prior to use.

Characterization

Thermogravimetric analysis. TGA was performed using a TA Instruments TGA 2050 thermogravimetric analyzer operated at a heating rate of 20 °C min⁻¹ from room temperature to 800 °C under a continuous flow of air.

Differential Scanning Calorimetry. DSC was performed using a TA DSC-Q20 controller operated under an atmosphere of dry N_2. The samples were weighed (*ca.* 5–10 mg), sealed in an aluminium pan, and then heated from −40 to +250 °C at a scan rate of 20 °C min⁻¹. The glass transition temperature was taken as the midpoint of the heat capacity transition between the upper and lower points of the deviation from the extrapolated glass and liquid lines.

Small and Wide-Angle X-ray Scattering (SAXS and WAXS). SAXS data were collected using the BL17A1 wiggler beamline of the National Synchrotron Radiation Research Center (NSRRC), Taiwan. The samples were sealed between two Kapton windows (thickness: 12 μm) and measured at room temperatures. An X-ray beam having a diameter of 0.5 mm and a wavelength (λ) of 1.1273 Å was used for the SAXS measurement (Q range: 0.015–0.3 Å⁻¹). The Q values of the SAXS profiles were calibrated using a polyethylene standard, Ag behenate, and tripalmitate. WAXS spectra of powders were obtained using a Rigaku D/max-2500 X-ray diffractometer. The radiation source was Ni-filtered Cu Kα radiation at a wavelength of 0.154 nm. The voltage and current were set at 30 kV and 20 mA respectively. The sample was mounted on a circular sample holder; the data were collected using a proportional counter detector over the $2d$ range from 2 to 50° at a rate of 5° min⁻¹. Bragg's law ($\lambda = 2d \sin \theta$) was used to compute the d-spacing corresponding to the complementary behavior.

Transmission Electron Microscopy. Transmission Electron Microscopy (TEM) was performed using a JEOL JEM-1200CX-II microscope operated at 120 kV. To stain the hydrophilic domains, the membrane was converted into its Pb^{2+} form through immersion in 1 N $Pb(OAc)_2$ solution overnight and then rinsed with water. For TEM observation, the ultra-microtome section of the dried membrane (50 nm slices) was placed on 200 mesh copper grids.

Conductivity and related measurements. The frequency-dependent impedance properties (from 10 kHz to 10 Hz) of the thin films were measured using an Autolab apparatus (Eco Chemie). For conductivity measurements, the membrane was placed in a conductivity cell between stainless-steel blocking

electrodes at 30–70 °C under 90% humidity. The conductivity was calculated according to the equation:

$$\sigma = \frac{L}{AR_b} \quad (1)$$

where σ is the conductivity, L is the membranes thickness, A is the section area of the stainless-steel electrode, and R_b is the bulk resistance. The measured conductivity was characterized following procedures described previously.[16]

Water uptake and related measurements. The water uptake (WU), number of water molecules per ionic group (λ), bound water ratio, and ion exchange capacity (IEC) were all measured and calculated as described previously.[13–15]

The water uptake (WU, %) was calculated using the equation:

$$WU(\%) = \frac{W_{wet} - W_{dry}}{W_{dry}} \times 100\% \quad (2)$$

where W_{wet} and W_{dry} are the wet and dry weights of the membrane, respectively. The completely dried proton exchange membrane (PEM) was immersed in deionized water at room temperature for 24 h, then removed quickly and blotted with filter paper to remove any excess water on the membrane surface, and immediately weighed to obtain its wet mass (W_{wet}). The dried weight of the membrane was measured after drying at 120 °C for 24 h.

The ion exchange capacity (IEC) was determined through titration with NaOH solution of the acid released after immersing the membrane (in its acid form) into 1 M NaCl solution.[14] The ionic concentration was calculated using the equation:

$$[H^+] = \frac{IEC \times W_d / V_w}{1000} \quad (3)$$

where IEC refers to the titrated IEC, W_d is the weight of the dried membrane, and V_w is the volume of the wet membrane.

Acknowledgements

Notes and references

1 (a) L. Brunsveld, B. J. B. Folmer, E. W. Meijer and R. P. Sijbesma, *Chem. Rev.*, 2001, **101**, 4071; (b) J. L. Sessler, C. M. Lawrence and J. Jayawickramarajah, *Chem. Soc. Rev.*, 2007, **36**, 314.
2 W. H. Binder and R. Zirbs, *Adv. Polym. Sci.*, 2007, **207**, 1.
3 (a) C. R. South, C. Burd and M. Weck, *Acc. Chem. Res.*, 2007, **40**, 63; (b) M. Muthukumar, C. K. Ober and E. L. Thomas, *Science*, 1997, **277**, 1225.
4 R. Hoogenboom, D. Fourniera and U. S. Schubert, *Chem. Commun.*, 2008, 155.
5 A. J. Wilson, *Soft Matter*, 2007, **3**, 409.
6 (a) J. Choi, S. G. Kim and R. M. Laine, *Macromolecules*, 2004, **37**, 99; (b) J. Choi, A. F. Yee and R. M. Laine, *Macromolecules*, 2004, **37**, 3267; (c) R. Tamaki, J. Choi and R. M. Laine, *Chem. Mater.*, 2003, **15**, 793; (d) A. R. Bassindale, Z. Liu, I. A. MacKinnon, P. G. Taylor, Y. Yang, M. E. Light, P. N. Horton and M. B. Hursthouse, *Dalton Trans.*, 2003, 2945.
7 (a) L. Zhang, H. C. L. Abbenhuis, Q. Yang, Y.-M. Wang, P. C. M. M. Magusin, B. Mezari, R. A. van Santen and C. Li, *Angew. Chem., Int. Ed.*, 2007, **46**, 5003; (b) S. H. Phillips, T. S. Haddad and S. J. Tomczak, *Curr. Opin. Solid State Mater. Sci.*, 2004, **8**, 21; (c) E. Jeoung, J. B. Carroll and V. M. Rotello, *Chem. Commun.*, 2002, 1510; (d) D. Neumann, M. Fisher, L. Tran and J. G. Matisons, *J. Am. Chem. Soc.*, 2002, **124**, 13998.
8 (a) G. Wu and Z. Su, *Chem. Mater.*, 2006, **18**, 3726; (b) S.-Y. Lu and I. Hamerton, *Prog. Polym. Sci.*, 2002, **27**, 1661.
9 (a) E. Wang, P. Shi and Y.-W. Chang, *Rare Met.*, 2006, **25**, 224; (b) C. Hartmann-Thompson, A. Merrington, P. I. Carver, D. L. Keeley, J. L. Rousseau, D. Hucul, K. J. Bruza, L. S. Thomas, S. E. Keinath, R. M. Nowak, D. M. Katona and P. R. Santurri, *J. Appl. Polym. Sci.*, 2008, **110**, 958; (c) J. Choi, K.-M. Lee, R. Wycisk, P. N. Pintauro and P. T. Mather, *J. Electrochem. Soc.*, 2010, **157**, B914; (d) P. Chhabra and V. Choudhary, *J. Appl. Polym. Sci.*, 2010, **118**, 3013; (e) Y.-C. Yen, Y.-S. Ye, C.-C. Cheng, W.-Y. Chen, L.-D. Tsai, J.-M. Huang and F.-C. Chang, *Polymer*, 2010, **51**, 84.
10 Y.-S. Ye, Y.-J. Huang, C.-C. Cheng and F.-C. Chang, *Chem. Commun.*, 2010, **46**, 7554.
11 C.-C. Cheng, Y.-C. Yen and F.-C. Chang, *Macromol. Rapid Commun.*, 2011, **32**, 927–932.
12 I. Honma and M. Yamada, *Bull. Chem. Soc. Jpn.*, 2007, **80**, 2110.
13 (a) M. Zhai, S. Hasegawa, J. Chen and Y. Maekawa, *J. Fluorine Chem.*, 2008, **129**, 1146; (b) M. Zhai, J. Chen, S. Hasegawa and Y. Maekawa, *Polymer*, 2009, **50**, 1159; (c) O. A. Baturina, S. R. Aubuchon and K. J. Wynne, *Chem. Mater.*, 2006, **18**, 1498; (d) P. Colomban and A. Novak, Proton Conductors: Classification and Conductivity, in *Proton Conductors*, ed. P. Colomban, Cambridge University Press, UK, 1992, pp. 38–55.
14 (a) W. F. Chen and P. L. Kuo, *Macromolecules*, 2007, **40**, 1987; (b) M. L. D. Vona, D. Marani, C. D'Ottavi, M. Trombetta, E. Traversa, I. Beurroies, P. Knauth and S. Licoccia, *Chem. Mater.*, 2006, **18**, 69; (c) Z. W. Chen, B. Holmberg, W. Z. Li, X. Wang, W. Q. Deng, R. Munoz and Y. S. Yan, *Chem. Mater.*, 2006, **18**, 5669.
15 (a) D. S. Kim, G. P. Robertson and M. D. Guiver, *Macromolecules*, 2008, **41**, 2126; (b) Y. W. Kim, J. K. Choi, J. T. Park and J. H. Kim, *J. Membr. Sci.*, 2008, **313**, 315; (c) Z. Zhou, R. Liu, J. Wang, S. Li, M. Liu and J. L. Bredas, *J. Phys. Chem. A*, 2006, **110**, 2322.
16 Y. S. Yea, W. Y. Chen, Y. J. Huang, M. Y. Cheng, Y. C. Yen, C. C. Cheng and F. C. Chang, *J. Membr. Sci.*, 2010, **362**, 29.